Development, Verification and Application of the SNL-SWAN Open Source Wave Farm Code

K. Ruehl[#1], A. Porter[2*], C. Chartrand[3#], H. Smith[4+], G. Chang[5^], J. Roberts[6#]

[#]*Sandia National Laboratories*
Albuquerque, NM, USA
[1] kmruehl@sandia.gov
[3] ccchart@sandia.gov
[6] jdrober@sandia.gov

[*]*Coast & Harbor Engineering*
Edmonds, WA, USA
[2] aaronp@coastharboreng.com

[+]*University of Exeter*
Exeter, UK
[4] H.C.M.Smith@exeter.ac.uk

[^]*Integral Consulting Inc.*
Santa Cruz, CA USA
[5] gchang@integral-corp.com

Abstract— **The lack of deployed wave farms means direct measurement of the effects of Wave Energy Converter (WEC) arrays on near-field and nearshore wave propagation is not possible. As a result, environmental impacts of wave farms are largely determined through simulations using numerical wave models. Sandia National Laboratories has developed the SNL-SWAN code, an open source wave farm code that has been modified to more accurately model WECs by accounting for device specific power performance. The work presented in this paper demonstrates the development, verification, preliminary validation, and application of the SNL-SWAN code.**

Keywords— **wave energy, wave farm, WEC array, spectral models, open source**

I. Introduction

In order for ocean wave energy to become a commercially viable technology, wave energy converters (WECs) will necessarily be deployed in wave farms, or arrays of multiple WECs. It is likely that these wave farms will consist of tens or hundreds of WECs, with the potential for affecting nearshore wave propagation and circulation; thus modifying sediment transport patterns. Due to the lack of deployed wave farms, direct measurement of the effects of WEC arrays on near-field and nearshore wave propagation is not possible. As a result, potential environmental effects must be evaluated using numerical models to assess potential environmental effects. SNL-SWAN (Sandia National Laboratories – Simulating WAves Nearshore) [1] is a version of the TU Delft spectral wave model SWAN [2], modified to include a WEC Module for better modeling WECS, and thus wave farms. SNL-SWAN improves the capability to estimate near-field and nearshore wave climate impacts due to WECs, by accounting for device specific power performance in the code. In SNL-SWAN, the amount of energy extracted at the WEC location is determined from user-supplied WEC power performance data. Using the WEC module, the WEC's energy extraction can be applied based on the WEC power performance data at the peak period, as a function of incident wave periods, or as a function of both incident wave periods and wave heights. In addition to estimating potential environmental effects, the SNL-SWAN code outputs WEC power at each location, and can be used for preliminary wave farm optimization.

II. Background

Due to the lack of deployed wave farms, and the desire to understand potential environmental effects, there has been extensive work on the modeling of wave farms by the wave energy community. Folley et al. provided a comprehensive overview of the different numerical approaches to model wav farms, and weighs their strengths and limitations [3]. Listed by Folley et al. 2012 as the numerical approaches to model wave farms are: potential flow models, Boussinesq/mild-slope wave models, spectral wave models, and CFD models. Troch et al. 2013 ran wave tank experiments of a 25 WEC array, measuring the device response and resulting modifications to the wave field as part of the WECwakes project [4]. Carballo and Iglesias 2013 performed wave tank experiments on the WaveCat to determine the transmission and reflection coefficients for (baseline) SWAN simulations [5]. These SWAN simulations were used to assess the environmental impact of deploying a wave farm of 12 WaveCats off the coast of Spain. Smith 2012 et al. analysed the impact of wave farms deployed at the WaveHub site using a modified version of the SWAN code accounting for the frequency- and directional-dependent energy extraction of WECs [6]. Silverthorne and Folley 2011 implemented modifications in TOMAWAC to account for the frequency and directional dependent energy extraction of WECs [7]. Recently DNV-GL developed the commercial code WaveFarmer to model wave farms [8]. The WaveFarmer planning tool uses both time-domain and spectral approaches to model wave farms, where the time-domain method implements WaveDyn, and the spectral method modifies the (baseline) TOMAWAC code to account for the frequency and directional dependent energy extraction of WECs [9]. With the exception of WaveFarmer, none of the

aforementioned numerical approaches have been validated by comparison to wave transformation through wave farms observed in a controlled or open ocean environment. The modifications made to the SNL-SWAN code are unique in that they have been extensively verified through numerical comparison, have been compared to experimental array tests, and the code is freely available to the open source community through GitHub [10].

As a follow on to the preliminary work on SNL-SWAN development presented at EWTEC in 2013 [11], this paper will provide an overview of the development, verification and application of the open source SNL-SWAN code. First the baseline SWAN code and SNL-SWAN code modifications will be described. Then a comparison of the SNL-SWAN code to related spectral wave models with a WEC component [6] [12], and to experimental data will be given. Finally, application of SNL-SWAN in an open ocean site will be presented.

III. Baseline SWAN Code

Simulating WAves Nearshore (SWAN) is an open source, third-generation wave model, developed at Delft University of Technology. Baseline SWAN models wave transformation to shore accounting for bathymetry, and physical processes such as shoaling, refraction, current, bottom friction, by solving the wave action balance equation with sources and sinks. For more information on the theory behind SWAN v41.01, refer to the SWAN manuals [2].

To model WECs in baseline SWAN, the OBSTACLE feature is used. The SWAN OBSTACLE is defined by a line crossing between two grid points, with a transmission coefficient, K_t., and a reflection coefficient, K_r. The transmission coefficient acts as an energy sink in the wave action balance equation, extracting a fraction of the incident wave energy, as shown in Eq. (1).

$$\begin{aligned}\left(\frac{1}{\Delta t}+\left(D_{x,1}+D_{x,2}\right)c^{+}_{x,i,,j}+\left(D_{y,1}+D_{y,2}\right)c^{+}_{y,i,,j}\right)N^{+}_{i,,j}\\ -\frac{N^{-}_{i,,j}}{\Delta t}-D_{x,1}\left(c_x{K_{t,1}}^2N\right)^{+}_{i-1,j}\\ -D_{y,1}\left(c_y{K_{t,1}}^2N\right)^{+}_{i-1,j}-D_{x,2}\left(c_x{K_{t,2}}^2N\right)^{+}_{i,j-1}\\ -D_{y,2}\left(c_y{K_{t,2}}^2N\right)^{+}_{i,j-1}=S^{+}_{i,j}\end{aligned} \quad (1)$$

The limitation of using this approach to model WECs is that the SWAN OBSTACLE formulation extracts a constant amount of energy from each incident wave period (or binned frequency). In reality, WECs are designed to extract more energy at some sea states, and less at others. Additionally, WECs are often controlled to maximize the energy extraction by tuning the WEC energy conversation with incident wave climate [13]. Due to the variety of existing WEC technologies, there is significant variation in the power performance of different devices due to factors such as: power rating, bandwidth, directional dependence, and control [14]. All of these factors influence the energy extraction of WECs, and thus the transformation of waves through WEC arrays and influence on near-field and far-field environmental effects. None of these factors are captured in the baseline SWAN formulation. To address this shortcoming, modifications were made to SWAN v41.01 (referred to as SNL-SWAN) to improve modeling of WECs will be described in the following section.

IV. SNL-SWAN Code Modifications

The development of the SNL-SWAN code was done iteratively by modifying the SWAN v41.01 with increasing feature complexity. The result of this effort is release of the SNL-SWAN v1.0 open source code, available on GitHub [10]. The description that follows is in reference to the v1.0 release version, and does not include feature additions planned for future releases (this is covered in the future work section).

SNL-SWAN v1.0 incorporates a WEC Module with five different options (referred to as OBCASE) that modify the baselines SWAN OBSTACLE formulation, a summary of which is shown in Table I. The first option, OBCASE 0, is the baseline SWAN OBSTACLE formulation, described in the previous section. The other four options have modified the baseline SWAN OBSTACLE formulation to calculate the transmission coefficient, K_t defined in Eq. (1), based on user-defined WEC power performance data. OBCASE 1 and 3 calculate K_t^2 based on a user-defined power matrix, and OBCASE 2 and 4 calculate K_t^2 based on a user-defined relative capture width (RCW) curve. Power matrices and RCW curves were chosen as the methods to define WEC power performance because they are metrics commonly used by industry to assess WEC performance.

Table I - Summary of SNL-SWAN WEC Module options

OBCASE	DESCRIPTION
0	Baseline SWAN formulations using constant K_t^2 value, specified by user in INPUT file.
1	WEC power matrix used to calculate K_t^2, applied as a constant value across all frequencies.
2	WEC RCW used to calculate K_t^2, applied as a constant value across all frequencies.
3	WEC power matrix used to calculate K_t^2, applied as a unique value at each binned frequency.
4	WEC RCW used to calculate K_t^2, applied as a unique value at each binned frequency.

The difference between these options is how they calculate and apply the transmission coefficients. For OBCASE 1 and 2, the transmission coefficient is calculated based on the WEC power performance at the peak wave period of the incident wave climate, Tp, and applied as a constant transmission coefficient across all binned frequencies. For OBCASE 3 and 4, the transmission coefficient is calculated based on the WEC power performance at each of the binned incident wave climate frequencies, and applied as a unique transmission coefficient at each binned frequency. Figure 1 shows a conceptual comparison of the difference between OBCASE 2 and OBCASE 4. For OBCASE 1, the resulting spectrum (shown in red) is the same shape as the incident spectrum (shown in black) because they apply a constant extraction

term across all frequencies. Alternatively, for OBCASE 4 the resulting spectrum (shown in blue) does not match the shape of the incident spectrum. This is because a different amount of energy was extracted per each binned frequency.

The modifications made to SNL-SWAN allow the code to calculate realistic energy extraction terms based on existing WEC power performance data, and to address changes in spectral shape due to WEC power extraction. The implication of the code modifications is that wave farms will be more realistically modelled, resulting in more confidence in the observed environmental effects from deployment of WEC arrays.

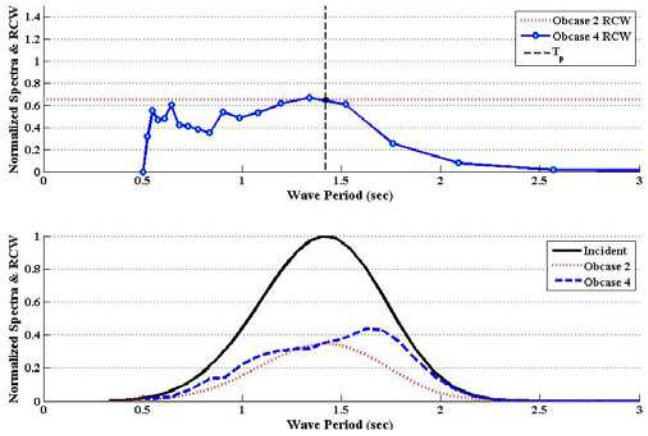

Figure 1 – OBCASE conceptual comparison visualization

V. Verification and Validation

A critical step in any code development project is verification and validation. This is especially true for codes such as SNL-SWAN that are used to model WEC arrays and predict environmental effects in lieu of direct measurements from wave farm deployments. In the following sections, description of SNL-SWAN verification by comparison to related spectral wave models will be given. Additionally, preliminary validation of the code will be presented by comparison of SNL-SWAN simulations to the WEC array experimental data gathered by Columbia Power Technologies at Oregon State University [15].

A. Code-to-code Comparison

An earlier modification to SWAN to enable frequency-dependent energy absorption was implemented by the University of Exeter in 2008. The modified code, Exeter Modified SWAN (EMS), incorporates an optional enhancement to the OBSTACLE command in SWAN. The modified command, OBSTACLE WEC_OMNI, allows the energy transmission to be defined at each spectral frequency, thereby permitting variable energy transmission across the spectrum.

A more detailed description of the code modifications can be found in Smith et al., 2012. However, one of the key differences between the implementations of SNL-SWAN and EMS lies in the representation of the variable energy transmission through an obstacle. EMS requires a power transmission coefficient, defined as per the standard SWAN definition of the ratio of transmitted significant wave height, $H_{m0,t}$, to incident $H_{m0,i}$, to be calculated for each spectral frequency in a particular SWAN run. The power transmission coefficient at a given frequency can be calculated from the device response function, i.e. the varying power capture of the device with frequency, via a power transfer function (PTF) curve, which defines the proportion of extracted, or absorbed, power at each frequency. The proportion transmitted by the obstacle is therefore calculated as 1-PTF(f). Since power is proportional to the square of H_{m0}, the SWAN transmission coefficient at each frequency, $K_t(f)$, is calculated as $(1-PTF(f))^{0.5}$. In practice, the PTF is equivalent to the SNL-SWAN relative capture width, with the key difference in the SNL-SWAN usage being that relative capture width is defined as a function of wave period rather than frequency. Results obtained using EMS should therefore be equivalent to those found using SNL-SWAN OBCASE 4.

This equivalence was tested in a direct comparison study between the two codes. Tests were run over a 2000 x 2000m deepwater grid with 100m resolution to compare the basic functionality of both codes. A barrier was established from north to south along the centre line of the grid. Transmission characteristics were applied, with full transmission ($K_t = 1$) at all frequencies except four, where total blockage was applied ($K_t = 0$).

The output spectra at a location 100m behind the centre point of the barrier are shown in Figure 2 for both codes. As would be expected, the resultant spectral densities, S(f), at the frequencies where transmission was set to zero are also zero, or very close to it. A visual assessment indicates near-identical results obtained with the two codes. The differences in the spectral densities between the codes were calculated and illustrated in the third plot in Figure 2 to ascertain their extent. Although small, differences are seen at frequencies of 0.0902Hz, 0.0988Hz, 0.1295Hz and 0.1418Hz. These are the frequencies where the transmission was set to zero in the EMS case. When the RCW curve was constructed for the SNL-SWAN case, the frequencies were converted to periods and these were then interpolated by SNL-SWAN, leading to the small differences.

These results indicate that the two modified versions of the code are providing the same functionality, despite their different implementations.

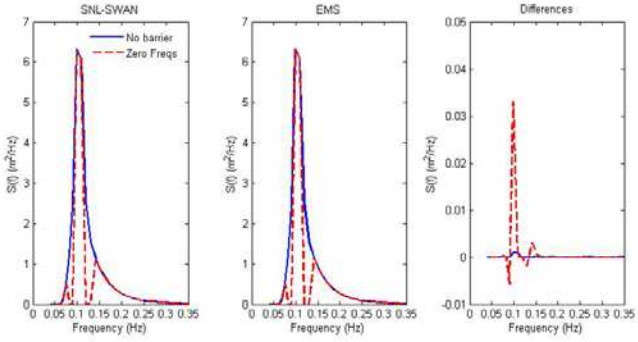

Figure 2 – SNL-SWAN and EMS runs with/without an obstacle (obstacle has total blockage at four frequencies/periods only). Differences in the results between the two codes are shown in the third plot, with positive values indicating larger spectral densities obtained using EMS.

B. Experimental Comparison

Performance of SNL-SWAN is validated through comparison to the experimental array tests of the Columbia Power Technologies' (ColPwr) Manta 3.1 WEC device performed at Oregon State University's Hinsdale Directional Wave Basin (DWB). The WEC array experiments consisted of trials with up to five, 1:33 scale "Manta 3.1" WECs moored in the in the DWB. Arrays of 1, 3 and 5 WECs were tested with a variety of wave conditions, in both regular waves and with representative wave climates. Information on these experiments is available in greater detail in Haller 2011 and Porter 2012. In order to compare the numerical results from SNL-SWAN model directly to experiments, a Directional Wave Basin model domain was developed from measured bathymetry and basin dimensions. Data output from the numerical model trials can be compared to data points at the locations of the wave gauges used in the experiments, see Figure 2.

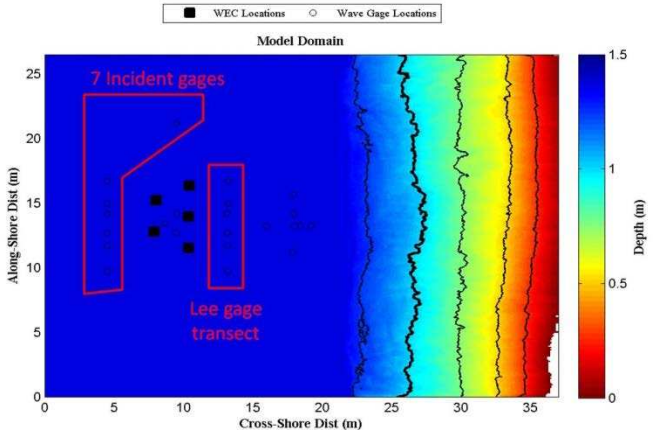

Figure 3 - Numerical Modelling domain with wave gage locations overlaid.

This validation effort focuses on six sea states with directional spreading enabled (s = 4), for the 5-WEC array arrangement due to the highest signal-to-noise ratio in the data. These sea states are summarized below in Table II. Previous work has shown that with directional spreading enabled SWAN simulates the shape of the apparent wave shadow (reduction in wave heights) due to the presence of a single WEC approximately the same with diffraction on, as with diffraction off [16]. In these model simulations diffraction was not enabled.

Table II - Experimental Sea States

Sea State	Directional Spreading	Hs Target (model)	Tp target (model)	Hs Target (field)	Tp target (field)
HI	Off, On	4.5cm	1.22 sec	1.5m	7 sec
OR2	Off, On	7.6cm	1.42 sec	2.5m	8.2sec
OR1	Off, On	4.5cm	1.62 sec	1.5m	9.3 sec
IR	Off, On	10.6cm	1.62 sec	3.5m	9.3 sec
OR3	Off, On	7.6cm	1.82 sec	2.5m	10.5sec
OR4	Off, On	7.6cm	2.22 sec	2.5m	12.8sec

For each of these trials WECs were simulated using Switch 4, as the RCW curve for the Manta 3.1 was provided by ColPwr. A power matrix was not generated during these tests. Results are shown in Figure 4for each sea state, and the black dashed line in the top left panel shows the transect location for model-data comparison. The RCW curve used in these simulations, and which was determined spectrally as a result of the trials is shown in relation to the six sea states in Figure 3. The RCW curve and the spectra have been normalized by the maximum values for simplicity. At this stage of analysis, and due to the size of the statistical error bars associated with the measured wave spectra, the incident wave spectra input to SWAN is the parameterized PM shape with the target peak period of the wave tank experiments. The experiments targeted the PM spectra, and analysis has shown that the measured spectra are of similar shape and peak period.

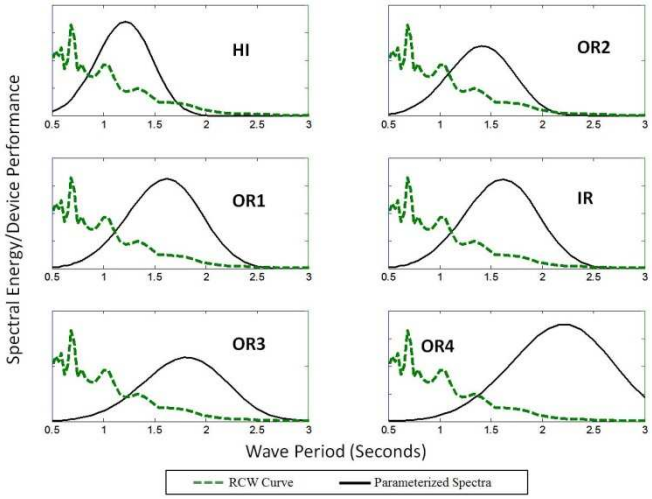

Figure 4 - RCW curve (green dashed) and normalized incident parameterized wave spectra (black) used in the SWAN simulations of the DWB trials.

Investigation of the data set showed variability of measured incident and lee (downwave of array) conditions. This experimental comparison investigates development of a validation procedure to incorporate measured wave variability. Incorporating variability of incident wave conditions is necessary to provide a range of possible incident conditions to SWAN, so that the validation procedure can incorporate such variability. That is, if the incident wave conditions in SNL-SWAN are not incorporating any potential variations, the results will not either.

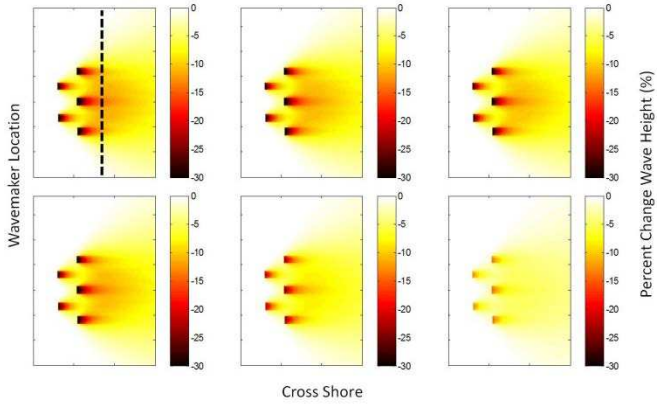

Figure 5 - Modelled change in wave height (darker colours indicate smaller wave heights) for the six sea states of interest.

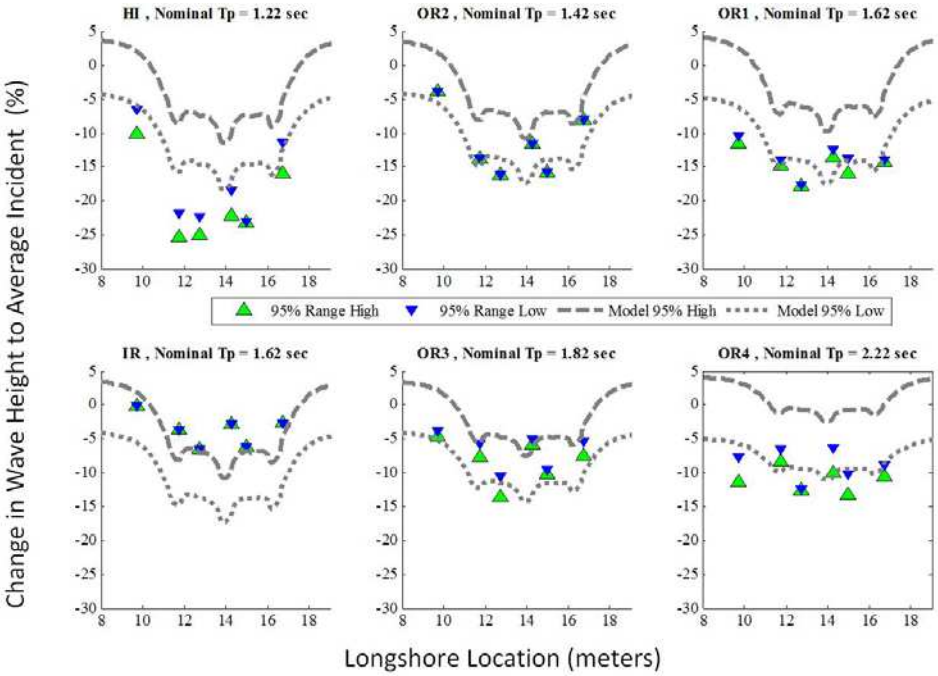

Figure 6 - Measured (triangles) and Modelled 95% confidence (grey dashed lines) wave height transects.

This work attempts consider both the variability of the measured incident significant wave height, and the variability of the measured significant wave height in the lee of the array. Because for each of the lee gages 1-3 trials (data points) of matching sea state conditions are available for the 5-WEC array size, this analysis will consider the minimum and the maximum measured significant wave height at each gage. At present, to minimize array effects on the measured incident wave conditions, and because limited empty tank trial tests were completed, the measured incident significant wave height are extracted from identical trials with 1-WEC in the water, as the ones compared to with 5 WECs in the water. For each sea state, the 95% confidence significant wave height was determined based on data from the seven incident wave gages over several trials (i.e., 7 gages, 3 trials, 21 data points). In this way the incident wave conditions input to SWAN bound the 95% confidence values for the incident wave height.

Using this procedure a comparison of modelled wave heights to measured wave heights is shown along the lee gage transect in Figure 5, which is located approximately 5 WEC diameters down wave of the edge of the average position of the WEC array. The x-axis in this figure is longshore location relative to the side of the wave basin. On the y-axis is the percent change as compared to the average incident wave height. The triangles represent the minimum and maximum recorded wave heights for gages in the lee array for the given sea state and 5-WEC array. In some cases, the minimum and maximum are equal due to only one trial being conducted for the given sea state and buoy arrangement (i.e. the up and down triangles are plotted atop each other). The wide dashed lines are model results for the +95% confidence interval incident wave heights, and the dotted line for the -95%.

The model results in Figure 5parameterize a range of likely wave shadowing considering measured variability of incident wave height. Model results show the anticipated degree of wave reduction due to power absorption by the WEC. In this case, the SNL-SWAN absorption option selected was Option 4, so the spectra are modified by a different amount at each frequency bin. In sea states OR1, OR2, OR3, and OR4, the degree of wave height reduction is reasonably similar in SNL-SWAN as in the experimental data, considering the range of possible incident wave conditions. In the Hawaii case (HI), the wave shadow appears to be under predicted, which may likely be due to short wave scattering, or tank limitations, as waves are shortest in this wave climate. For case IR, the largest differences between incident wave heights for the 1-WEC and 5-WEC cases appears to have occurred (not shown here). This may influence the comparison of wave heights between model (forced with parameterized incident conditions in 1-WEC cases), and measured (during 5-WEC cases). In summary, for the sea states with higher measures of repeatability between 1 and 5-WEC trials, SNL-SWAN simulates, near and within the 95% confidence level for incident wave conditions, the wave climate in the lee of the 5-WEC Array trials with this DWB/ColPwr data set.

VI. Modeling Open Ocean Wave Farm with SNL-SWAN

An overview of the application of the SNL-SWAN code to model a possible wave farm deployment site in Monterey Bay, CA is presented. An SNL-SWAN modeling sensitivity study was conducted to evaluate the effects of WEC and WEC array characteristics on nearshore wave propagation. A total of 288 model runs were conducted using SNL-SWAN switch 1, switch 2, switch 3, and switch 4, in which WEC device type [14], number of WECs in a WEC array, and WEC spacing in an array were varied according to Table 3. An additional set of baseline model runs was conducted without WECs.

Table III - SNL-SWAN model sensitivity analysis parameters

	WEC type
1	Small bottom-referenced heaving buoy (5 m*)
2	Bottom-fixed heave-buoy array[#] (5 m)
3	Bottom-referenced submerged heave-buoy[#] (7 m)
4	Floating heave-buoy array[%] (8 m)
5	Floating three-body oscillating flap device (9.5 m)
6	Floating two-body heaving converter (20 m)
7	Bottom-fixed oscillating flap (26 m)
8	Floating oscillating water column (50 m)
	Number of WECs
1	10
2	50
3	100
	WEC spacing x diameter (center-to-center)
1	4
2	6
3	8

*The published size is 3 m; 5 m was specified in SNL-SWAN due to limitations on computational grid size.
[#]Modelled as obstacles extending throughout the water column.
[%]Multi-body WEC modelled as a singular obstacle.

The model domain boundary wave conditions were determined from analysis of historical National Oceanographic and Atmospheric Administration National Data Buoy Center (NOAA NDBC) wave climatology records in Monterey Bay, CA. Initial significant wave height (H_s), peak wave period (T_p), and mean wave direction (MWD) were: H_s = 1.7 m, T_p = 12.5 s, and MWD = 205° for all 288 model runs. Note that the median wave direction calculated from the Monterey Bay NDBC buoy is 299°; however 205° was chosen such that wave shadowing effects for wave propagation to the Santa Cruz, CA coastline were minimized.

SNL-SWAN sensitivity analysis results included propagated wave heights, periods, and directions at all grid points within a nested model domain along the Santa Cruz, CA coastline. Additionally, model results were outputted at 18 specific model output points along the 30 m, 20 m, and 10 m depth contours in the Santa Cruz model domain. Sensitivity analysis results were evaluated in terms of percentage change from baseline, where baseline is model results in the absence of WECs; only wave height results are considered here.

Decreases in wave height were most sensitive to WEC power absorption as a function of incident wave height and period. This sensitivity was reflected not only in WEC device type model runs but also model runs that varied the number of WECs in an array (Figure 6). A larger number of buoys absorbed more power; therefore the larger the number of WECs in an array, the more wave height reduction was observed.

Model results were relatively insensitive to the spacing between WECs in an array except when the total WEC array footprint area was considered. When results were normalized by the array footprint area, wave height reductions decreased with increased WEC spacing (Figure 6). This implies that closely spaced WECs can result in potentially more decreased wave heights downstream of a WEC array as compared to WECs that are spaced farther apart, particularly for output locations that are directly in the lee of the WEC array.

Simulated wave heights decreased by up to 30% when comparing model runs with and without WECs. The largest decreases in wave height occurred when modeling an array of 100 bottom-fixed oscillating flap (B-OF) devices regardless of device spacing (Figure 7). The B-OF device power matrix was optimized for the modeled incident wave parameters as compared to the other modeled devices. Less than 15% differences in wave height in the presence and absence of WECs was determined for the other seven WEC device types.

The smallest percent change in wave height from baseline was found for the 5 m WECs. The largest WEC, the floating oscillating water column, did not result in the greatest reductions in wave height because its power matrix was not optimized at the incident wave height and period. However, decreases in wave height were observed over a larger area along the shoreline due to the WEC's larger size. As expected, wave height reductions were largest in the lee of the WEC array, along the WEC array centerline. Model output locations to the west and east showed negligible changes in wave height when compared to the baseline scenario.

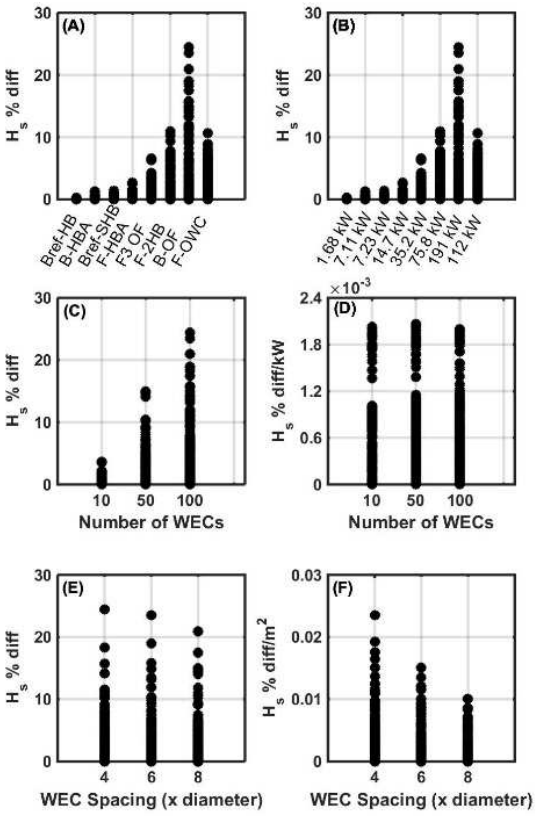

Figure 7 - Decreases in wave height as affected by variations in (A) WEC device type, (B) WEC average power absorption, (C) number of WECs in a WEC array, (D) number of WECs in an array considering the total absorbed power, (E) WEC spacing, and (F) WEC spacing considering the WEC array footprint area. Results are from SNL-SWAN switch 3 simulations.

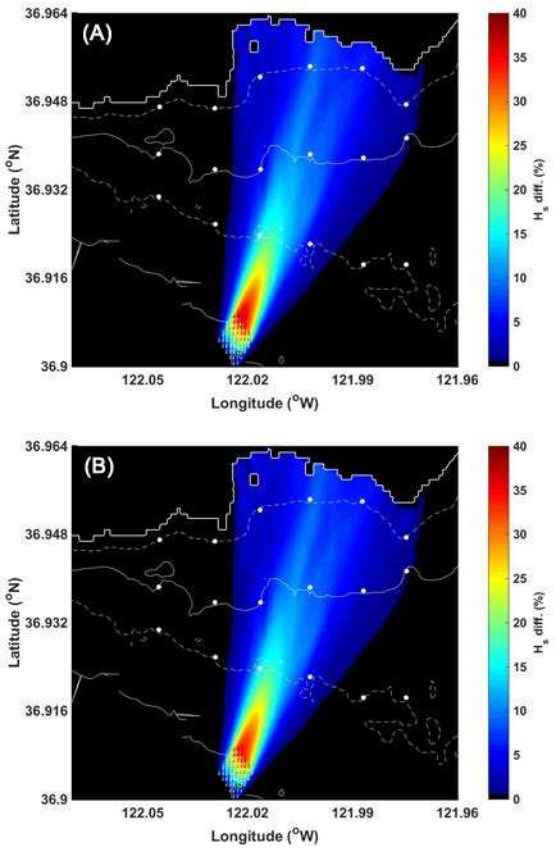

Figure 8 - Significant wave height percentage decrease (with WECs versus without WECs) using SNL-SWAN switch (A) 1 and (B) switch 3. Model runs specified 50 B-OF type WECs with 6 diameter spacing

In general, SNL-SWAN switch 2 and switch 4 model runs resulted in larger decreases in simulated wave height with WECs as compared to switches 1 and 3. This is likely due to data interpolation when calculating the RCW for switches 2 and 4. When comparing switches 1 and 2 versus switches 3 and 4 (i.e. constant frequency versus frequency-dependent transmission coefficients), less wave height reduction was observed when employing switches 1 and 2 as compared to switches 3 and 4 for smaller WECs (less than 10 m in diameter) with asymmetric power matrices. In other words, frequency-dependent transmission coefficients resulted in more power absorption for smaller WECs. In contrast, larger WECs with symmetrical power matrices resulted in less wave height reduction when modeled with switches 3 and 4 as compared to switch 1 or switch 2.

VII. Conclusions and Future Work

In conclusion, modifications to the open source spectral wave model, SWAN v41.04, have been made to more accurately model WECs. The result of this effort is SNL-SWAN v1.0, an open source code available on GitHub for direct download, or for further code development by the open course community. SNL-SWAN v1.0 includes a WEC module that accounts for the unique power performance characteristics of wave energy converters through user-defined power matrices or relative capture width curves. This functionality can either be implemented as a constant fraction of energy extraction across all wave periods (OBCASE 0 , 1, 2), or as a unique fraction of energy extraction at each binned incident wave frequency (OBCASE 3, 4). The SNL-SWAN code has undergone extensive verification by comparison to similar spectral models with a WEC component, and preliminary validation by comparison to experimental data.

Future work on this topic includes further modification of the SNL-SWAN code to include: outputting power at each WEC for unstructured grids, including a WEC frequency-dependent reflection term, and inclusion of binary (on/off) directional WEC power extraction. To provide input on additional features added to the SNL-SWAN code, please use the online questionnaire to provide feedback. SNL-SWAN v1.1 is planned for release in Fall 2015. The SNL-SWAN team also plans to further SNL-SWAN validation by extending the experimental data comparison to additional array testing data sets, from wave tanks and/or open ocean, pending availability.

Acknowledgment

This research was made possible by support from the Department of Energy's EERE Office's Wind and Water Power Technologies Office. The work was supported by Sandia National Laboratories, a multi-program laboratory managed and operated by Sandia Corporation, a wholly owned subsidiary of Lockheed Martin Corporation, for the U.S. Department of Energy's National Nuclear Security Administration under contract DE-AC04-94AL85000. Special thanks to Ken Rhinefrank and Pukha Lenee-Bluhm at Columbia Power Technologies for their characterization data of the Manta 3.1 WEC and Merrick Haller at Oregon State University for his guidance on using the experimental data.

References

[1] "Sandia National Laboratories: SNL-SWAN (Sandia National Laboratories – Simulating WAves Nearshore)." [Online]. Available: http://energy.sandia.gov/energy/renewable-energy/water-power/snl-swan-sandia-national-laboratories-simulating-waves-nearshore/.

[2] "TU Delft: SWAN." [Online]. Available: http://www.swan.tudelft.nl/.

[3] M. Folley, A. Babarit, B. Child, D. Forehand, L. O'Boyle, K. Silverthorne, J. Spinneken, V. Stratigaki, and P. Troch, "A Review of Numerical Modelling of Wave Energy Converter Arrays," in *Proceedings of the ASME 2012 31st International Conference on Ocean, Offshore and Arctic Engineering*, Rio de Janeiro, Brazil, 2012.

[4] P. Troch, V. Stratigaki, T. Stallard, D. Forehand, M. Folley, J. P. Kofoed, M. Benoit, A. Babarit, D. G. Sánchez, L. D. Bosscher, P. Rauwoens, B. Elsässer, P. Lamont-Kane, P. McCallum, C. McNatt, E. Angelelli, A. Pecher, E. C. Moreno, S. Bellew, E. Dombre, F. Charrayre, M. Vantorre, J. Kirkegaard, and S. Carstensen, "Physical Modelling of an Array of 25 Heaving Wave Energy Converters to Quantify Variation of Response and Wave Conditions," in *10th ewtec 2013 European Wave and Tidal Energy Conference Series*, Aalborg, 2013.

[5] R. Carballo and G. Iglesias, "Wave farm impact based on realistic wave-WEC interaction," *Energy*, vol. 51, pp. 216–229, Mar. 2013.

[6] H. C. M. Smith, C. Pearce, and D. L. Millar, "Further analysis of change in nearshore wave climate due to an offshore wave farm: An enhanced case study for the Wave Hub site," *Renew. Energy*, vol. 40, no. 1, pp. 51–64, Apr. 2012.

[7] K. E. Silverthorne and M. Folley, “A New Numerical Representation of Wave Energy Converters in a Spectral Wave Model,” in *EWTEC 2011*, Southampton, UK, 2011.
[8] J. Cruz, E. Mackay, M. Livingstone, and B. Child, “Validation of Design and Plannng Tools for Wave Energy Converters (WECs),” in *METS 2013*, Washington DC, 2013.
[9] B. F. M. Child and P. L. Weywada, “Verification and validation of a wave farm planning tool,” in *EWTEC 2013*, Aalborg, Denmark, 2013.
[10] *SNL-SWAN GitHub Release*. Sandia National Laboratories, 2014.
[11] K. Ruehl, Aaron Porter, Ari Posner, and Jesse Roberts, “Development of SNL-SWAN, a Validated Wave Energy Converter Array Modeling Tool,” in *Proceedings of EWTEC 2013*, Denmark, 2013.
[12] Aaron Porter, Kelley Ruehl, and Chris Chartrand, “Further Development of SNL-SWAN, a Validated Wave Energy Converter Array Modeling Tool,” in *Proceedings of the 2nd Marine Energy Technology Symposium*, Seattle, WA, USA, 2014.
[13] J. A. Oskamp and H. T. Özkan-Haller, “Power calculations for a passively tuned point absorber wave energy converter on the Oregon coast,” *Renew. Energy*, vol. 45, pp. 72–77, Sep. 2012.
[14] A. Babarit, J. Hals, M. J. Muliawan, A. Kurniawan, T. Moan, and J. Krokstad, “Numerical benchmarking study of a selection of wave energy converters,” *Renew. Energy*, vol. 41, pp. 44–63, 2012.
[15] M. Haller, A. Porter, P. Lenee-Bluhm, K. Rhinefrank, E. Hammagren, T. Ozkan-Haller, and D. Newborn, “Laboratory Observations of Waves in the Vicinity of WEC-Arrays,” in *EWTEC 2011*, Southampton, UK, 2011.
[16] A. Porter, “Laboratory Observations and Numerical Modeling of the Effects of an Array of Wave Energy Converters,” Oregon State University, Corvallis, Oregon, 2012.